Dual HDAC and PI3K inhibition abrogates NFκB- and FOXM1-mediated DNA damage response to radiosensitize pediatric high-grade gliomas

Sharmistha Pal, David Kozono, Xiaodong Yang, Wojciech Fendler, Whitney Fitts, Jing Ni, John A. Alberta, Jean Zhao, Kevin X. Liu, Jie Bian, Nathalene Truffaux, William A. Weiss, Adam C. Resnick, Pratiti Bandopadhayay, Keith L. Ligon, Steven G. DuBois, Sabine Mueller, Dipanjan Chowdhury, Daphne A. Haas-Kogan

Supplemental Figure:

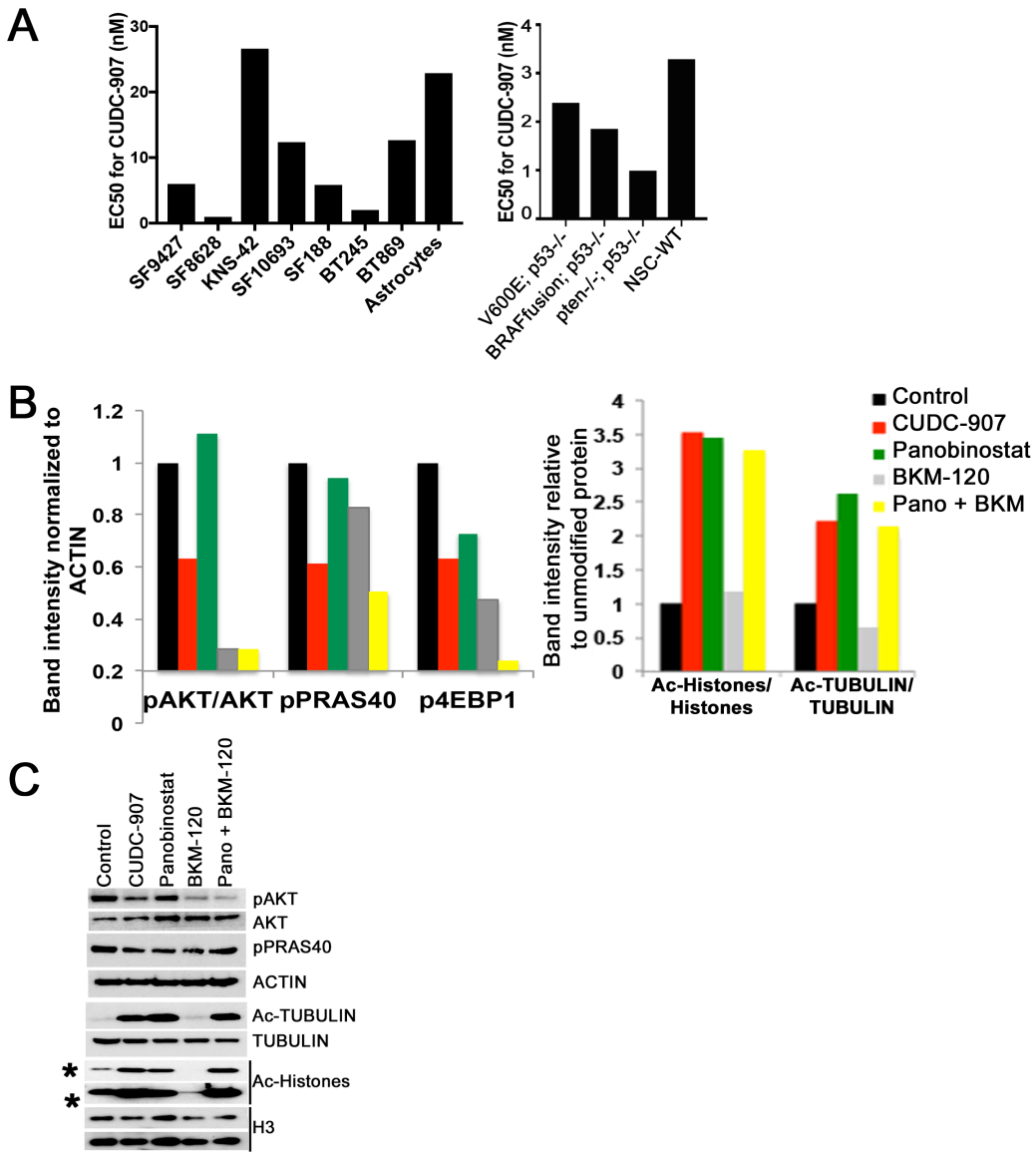

Supplementary Figure S1. CUDC-907 successfully inhibits HDAC and PI3K signaling, and exhibits single agent activity and synergism with radiation against pHGG and DIPG. (**A**) CUDC-907 concentrations required for 50% cell growth inhibition (EC_{50}) in glioma lines, normal human astrocytes, and normal mouse neural stem cells (NSC) as determined by PRISM using the data presented in Figure 1A and B. (**B**) ImageJ based quantification of Western blots in SF188 cells shown in Figure 1C. (**C**) Western blots analysis of SF8628 cells after CUDC-907 (100 nM), panobinostat (100 nM), or BKM120 (300 nM) or panobinostat (100 nM) plus BKM120 (300 nM) combination for either 2 hours for AKT, p-AKT, and acetylated proteins, or 16 hours for p-PRAS40. * indicates a shorter exposure time for the blot.

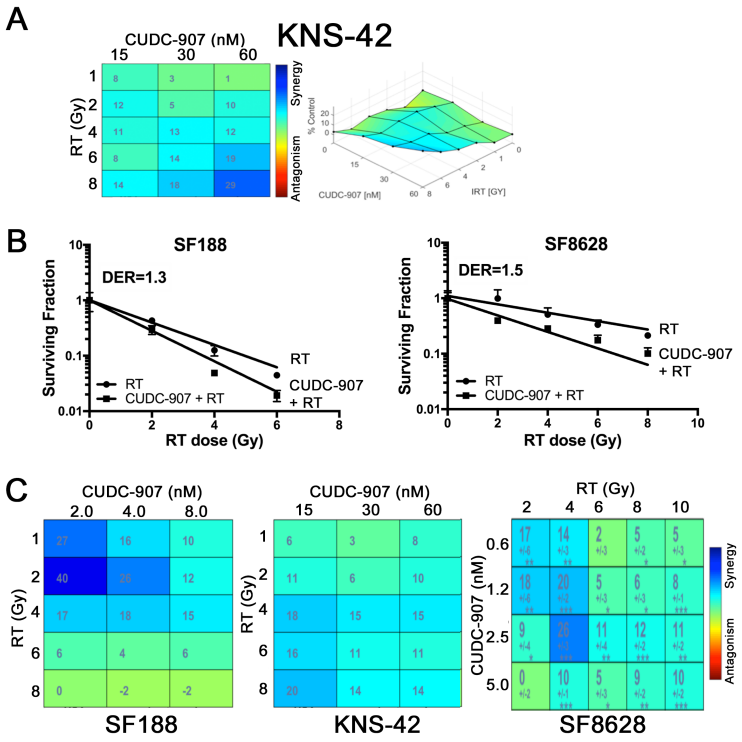

Supplementary Figure S2. CUDC-907 exhibits synergism with radiation against pHGG and DIPG. (**A**) KNS-42 cells treated with CUDC-907 at the indicated doses for 16 hours followed by irradiation; cell viability was measured 72 hours after CUDC-907 addition. Combenefit software analysis demonstrates synergism of CUDC-907 and radiation as indicated by the presence of blue-green. (**B**) Colonogenic cell survival assays were performed in triplicates and cells were treated with CUDC-907 (2 nM) for 16 hours prior to irradiation at various doses. Cells were allowed to form colonies (>50 cells) and stained with 0.1% crystal violet. Colonies were counted and surviving fractions are plotted. Data represent mean ± SEM. Dose enhancement ratios (DER) are calculated at 10% survival. (C) Synergistic cytotoxicity of CUDC-907 and radiation administered concurrently in SF188, KNS-42 and SF8628 cell lines. Cell viability was measured 72 hours after concurrent treatment and Combenefit software was used to analyze synergy-antagonism relationships.

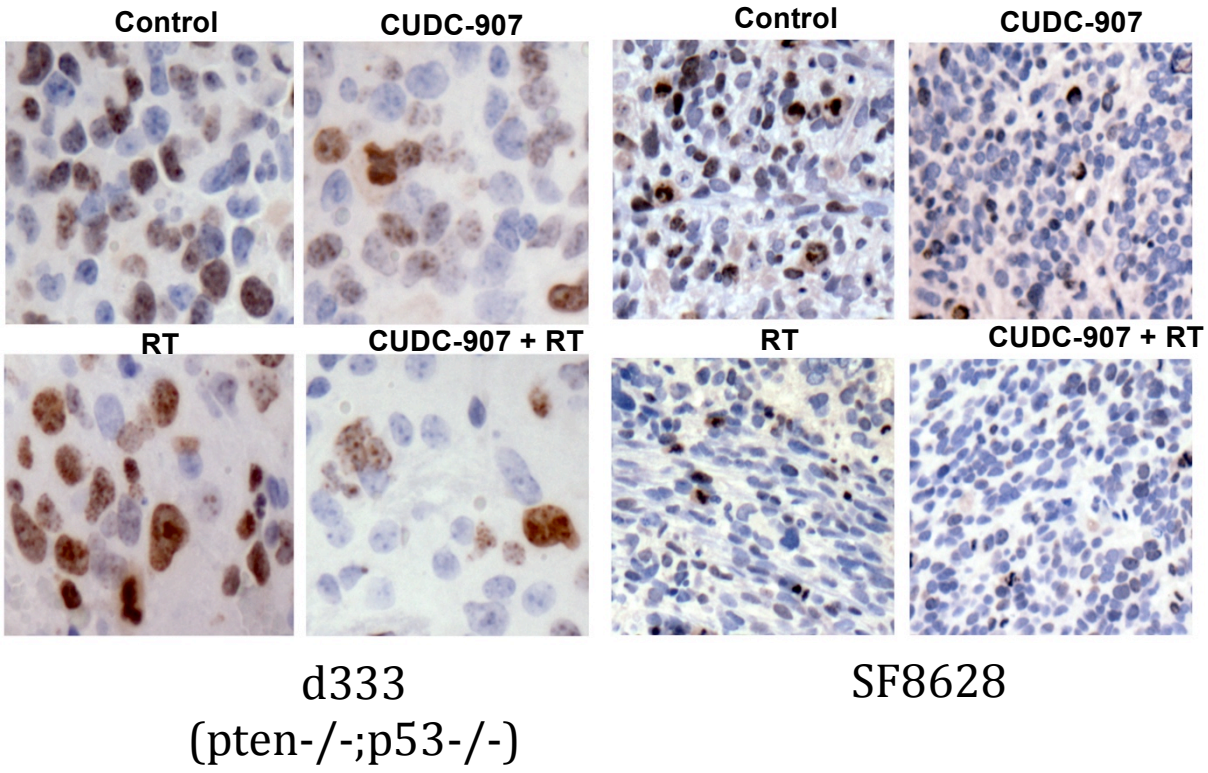

Supplementary Figure S3. Cell proliferation is reduced *in vivo* by CUDC-907 or irradiation (RT), with greater reduction after combination therapy compared to either single modality. Representative images of Ki-67 immunohistochemical staining of d333 (*pten*-/-;*p53*-/-) and SF8628 orthotopic tumors (quantification presented in Fig. 1F).

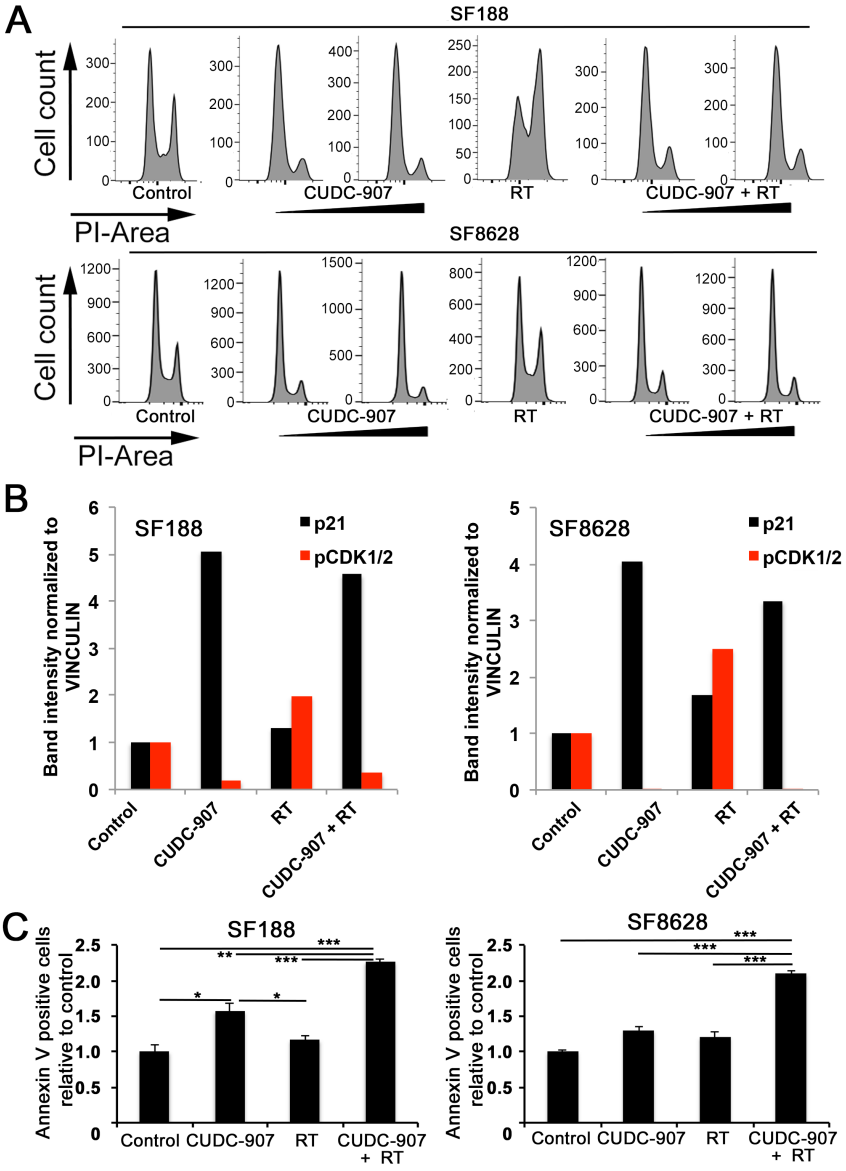

Supplementary Figure S4. CUDC-907 induces G1 cell cycle arrest and synergizes with radiation to induce apoptosis and alter cell cycle proteins. (A) Histograms representing the cell cycle profiles for the data presented in Figure 2A. (**B**) Quantitation of western blots shown in Fig. 2B using ImageJ software show induction of p21 and reduced phosphorylation of CDK1/2 in the presence of CUDC-907. (**C**) Apoptosis quantitated by Annexin V staining of SF188 and SF8628 following CUDC-907 (100 nM), radiation (4 Gy), or CUDC-907 followed 16 hours later by radiation. Annexin V positive cells were quantitated by flow cytometry, 4 hours after irradiation or 20 hours after CUDC-907 treatment. Statistical analyses with $p<0.05$ are indicated by *$p<0.05$, **$p<0.01$, ***$p<0.001$, ****$p<0.0001$.

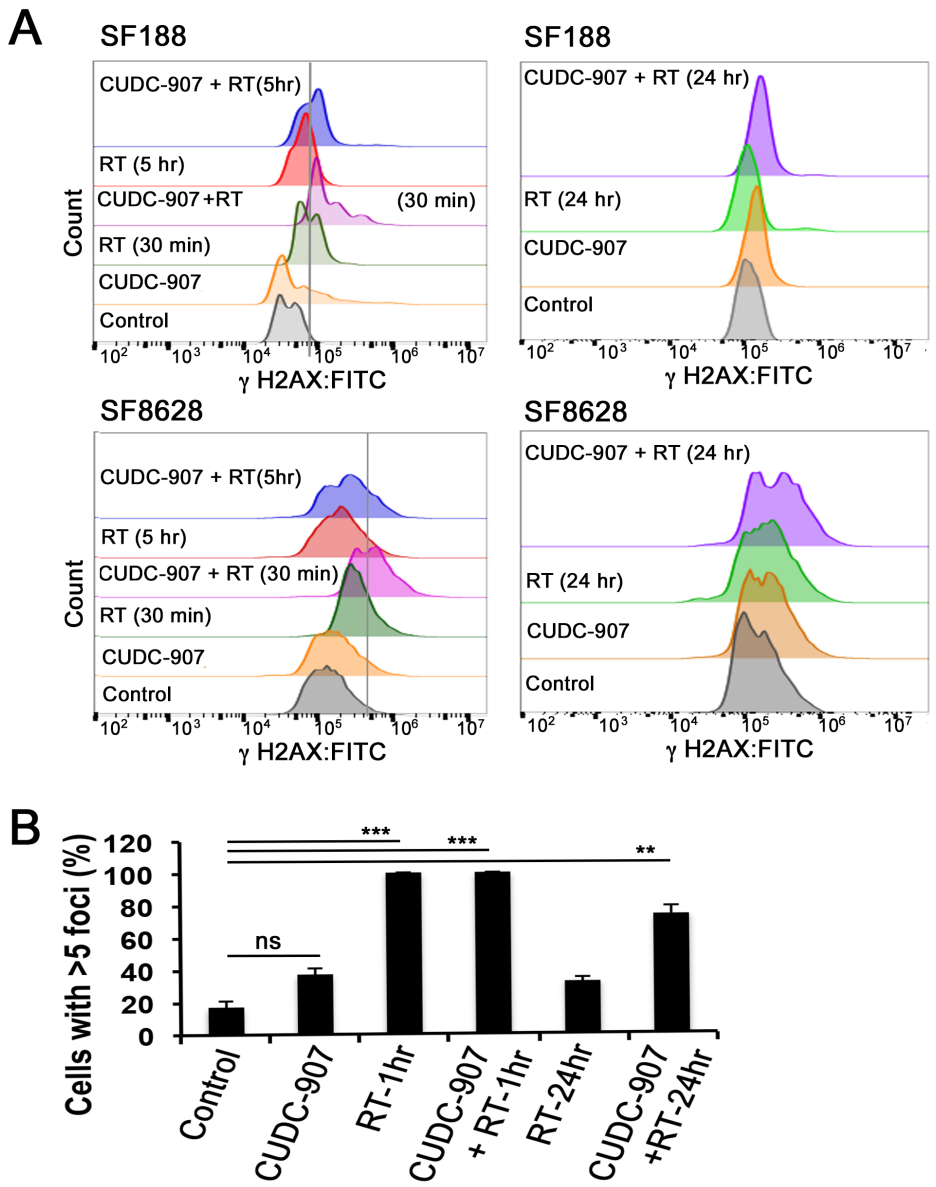

Supplementary Figure S5. CUDC-907 synergizes with radiation to induce DNA double strand breaks and delay DNA damage repair. (**A**) Flow cytometry histograms of anti-γ-H2AX staining following CUDC-907 (100 nM), radiation (4 Gy), or combination therapy, with quantitation presented in Figure 2D. Cells were fixed and stained 30 min, 5 hours, and 24 hours after radiation treatment. The 24-hour post-radiation time-point is compared to CUDC-907 treated cells that were grown under similar conditions without radiation exposure. (**B**) γ-H2AX foci visualized by immunoflourescence staining in SF188 cells treated with CUDC-907 (100 nM), radiation (4 Gy) or combination (CUDC-907 followed 16 hours later by radiation). A cell was considered positive if it contained ≥5 foci and at least 100 cells were imaged and counted per condition. All values are mean ± SEM and significant p values are shown as *p<0.05, **p<0.01, ***p<0.001, ****p<0.0001.

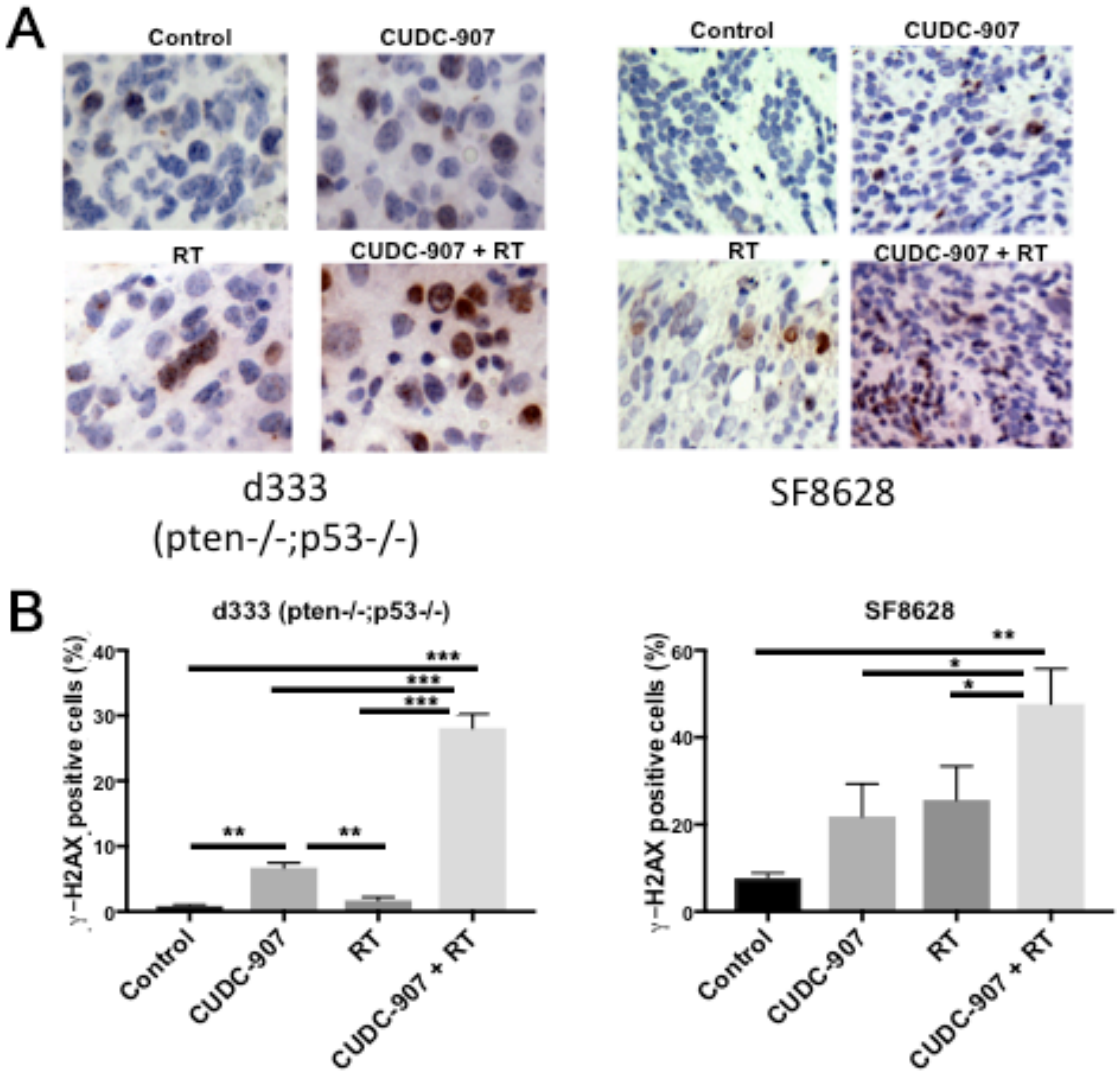

Supplementary Figure S6. CUDC-907 enhances radiation-induced DNA double strand breaks *in vivo*. γ-H2AX immunohistochemical staining of d333 murine gliomas and SF8628 DIPG model treated *in vivo* with CUDC-907 (100 mg/kg daily M-F), radiation (0.5 Gy M-W-F) or combination [CUDC-907 (100 mg/kg) following by radiation (0.5 Gy)]. The same murine brain sections were also stained for Ki-67 (data shown in Fig. 1F). (**A**) Representative images of γ-H2AX staining; (**B**) quantification of γ-H2AX IHC positive cells using Cell Profiler. Graph represents mean ± SEM and significant p values are indicated as *p<0.05, **p<0.01, ***p<0.001, ****p<0.0001.

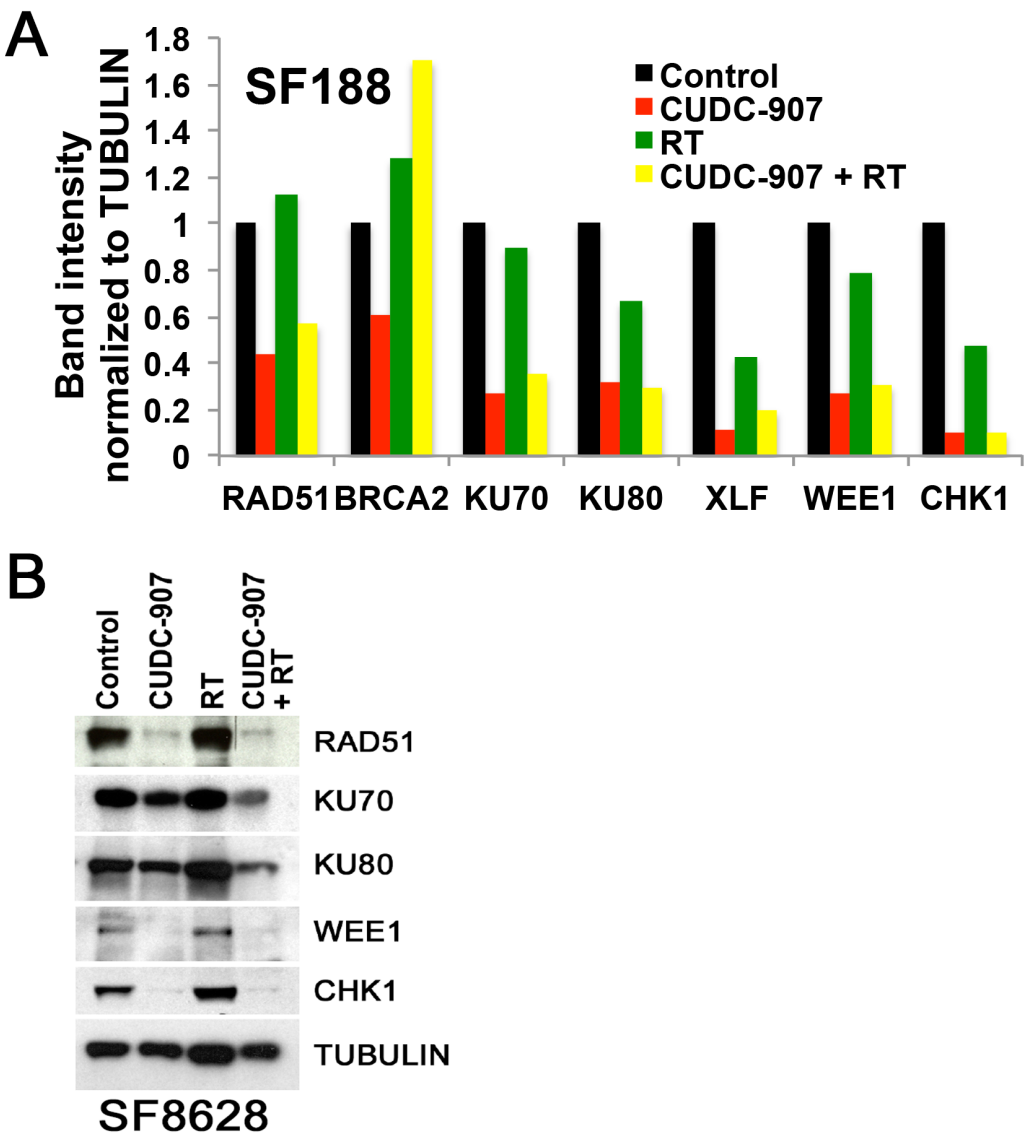

Supplementary Figure S7. CUDC-907 reduces expression of DNA damage response proteins. (**A**) Image J based quantitation of Western blots shown in Fig. 3E demonstrating reduced expression of HR, end joining, and checkpoint kinases after CUDC-907 treatment. (**B**) Western blot analyses following treatment of SF8628 DIPG cells with DMSO, CUDC-907 (100 nM), radiation (4 Gy) or combination (CUDC-907 followed 16 hours later by radiation).

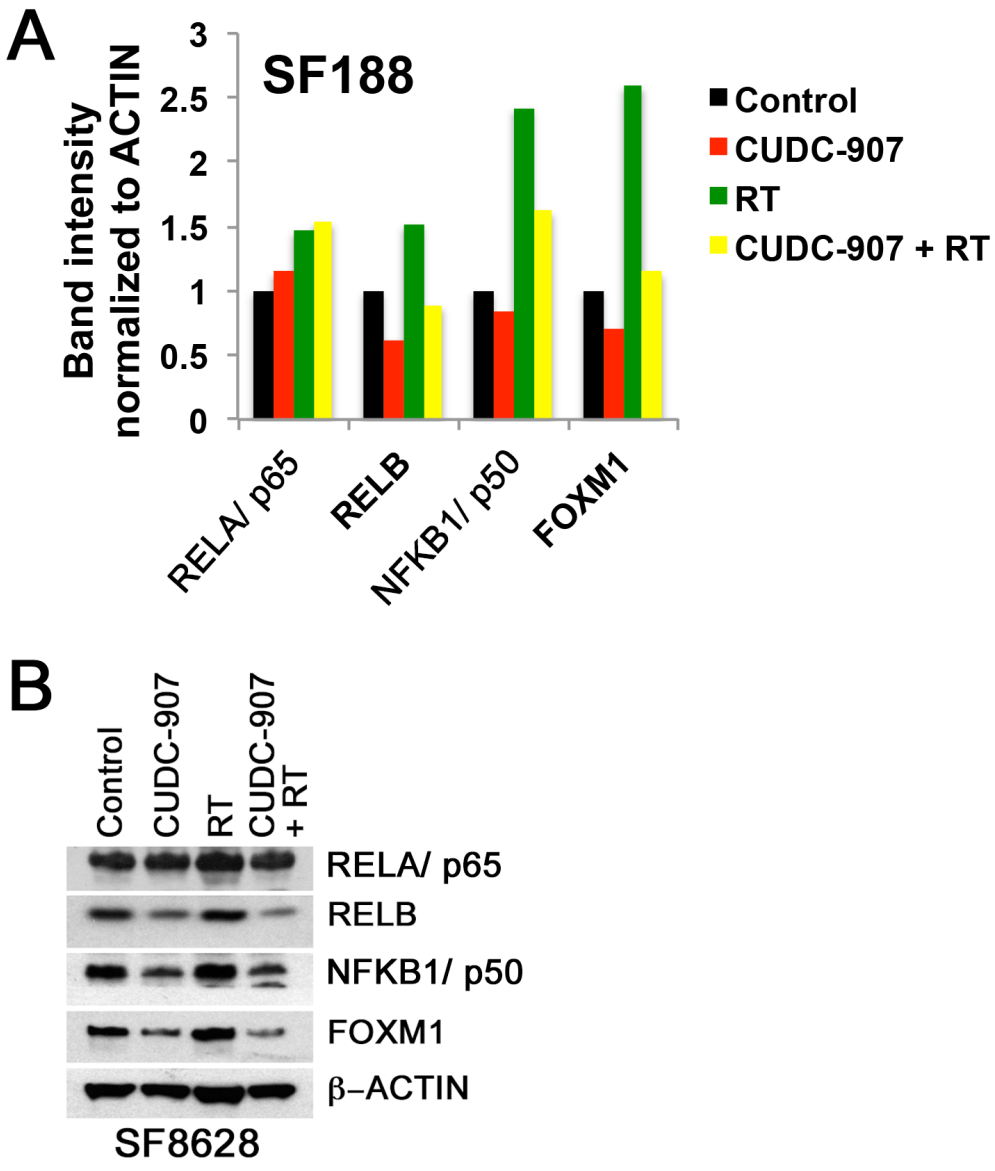

Supplementary Figure S8. CUDC-907 reduces expression of transcription factors, NFκB and FOXM1. (**A**) Western blot in Figure 4B is quantitated and graphs demonstrate reduced expression of p50/NFKB1, RELB and FOXM1 after CUDC-907 treatment and ablation of their upregulation by radiation when pretreated with CUDC-907. (**B**) Western blot analyses of the NFκB and FOXM1 proteins following treatment of SF8628 DIPG cells with DMSO, CUDC-907 (100 nM), radiation (4 Gy) or combination (CUDC-907 followed 16 hours later by radiation).

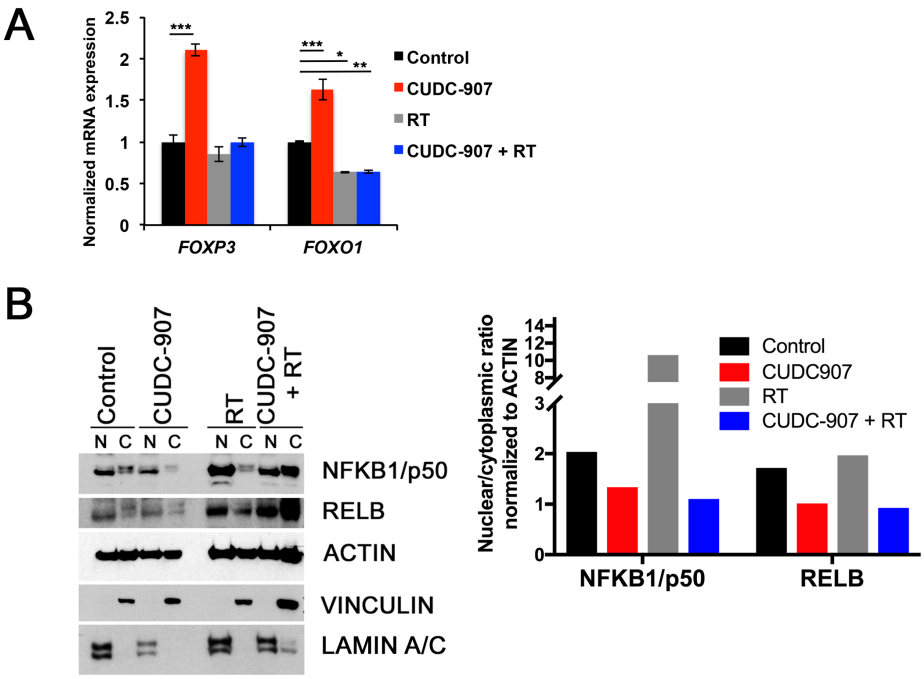

Supplementary Figure S9. CUDC-907 enhances forkhead genes, *FOXO1* and *FOXP3*, expression and impairs nuclear localization of NFKB1/p50 and RELB. (**A**) mRNA expression of two forkhead proteins, FOXO1 and FOXP3, analyzed by RT-qPCR following the indicated treatments, as in Fig. 4A. Significant p values are indicated as *p<0.05, **p<0.01, ***p<0.001, ****p<0.0001 (**B and C**) Western blot analysis of nuclear (N) and cytoplasmic (C) fractions and immunoflourescence staining for NFKB1/p50 and RELB in SF188 cells treated with CUDC-907 (100 nM), radiation (4 Gy) or combination (CUDC-907 followed 16 hours later by radiation). Western blots were quantitated using Image J software and the ratio of nuclear to cytoplasmic protein was determined after ACTIN normalization. VINCULIN and LAMIN A/C expression in cytoplasmic and nuclear fractions, respectively, demonstrate successful nuclear and cytoplasmic separation. For immunostaining, cells were fixed 1 hour after treatment and DAPI was used for nuclear counterstaining.

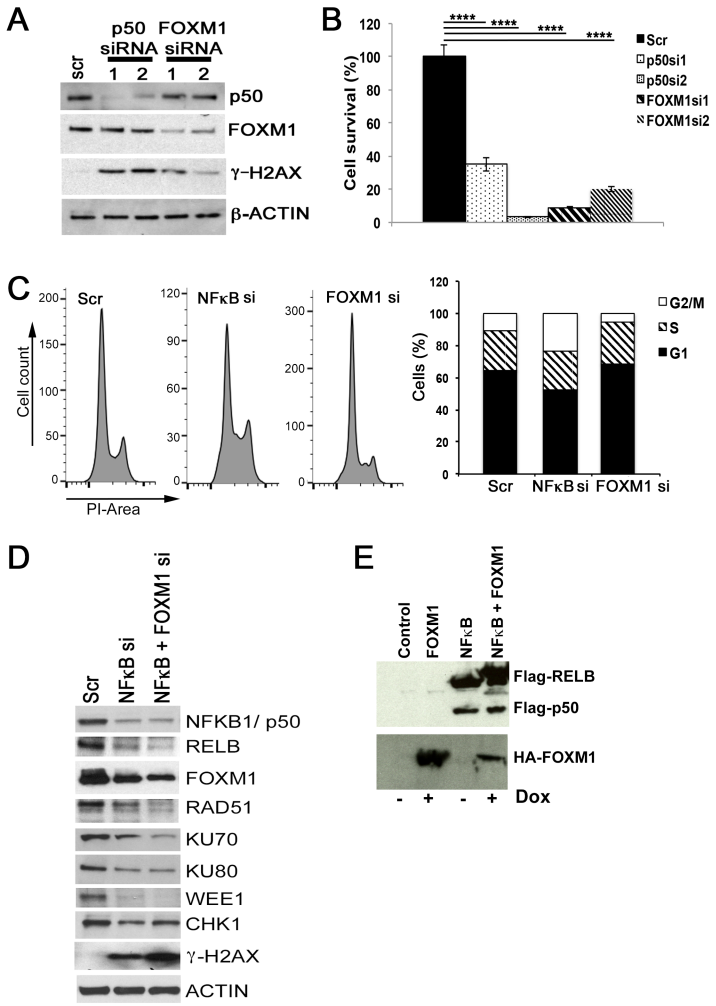

Supplementary Figure S10. Knockdown of NFκB and FOXM1 induces DNA damage, inhibits DNA damage response, and reduces cell survival. (**A**) Western blot analyses demonstrate knockdown of NFκB1/p50 and FOXM1 (using siRNA transfection for 72 hours) and induction of γ-H2AX, reflecting resultant DNA double strand breaks. (**B**) Knockdown of NFκB1/p50 or FOXM1 is cytotoxic and reduces cell viability in SF188 cells. Cells were transfected with the indicated siRNAs and cell viability was determined 72 hours post transfection by CellTiter-Glo assay. Statistical analyses are indicated as *p<0.05, **p<0.01, ***p<0.001, ****p<0.0001. (**C**) Cell cycle profiles of SF188 cells after 72 hours of siRNA-mediated knockdown of NFKB1/p50 and RELB (NFκB) or FOXM1. (**D**) NFκB and FOXM1 knockdown decreases expression of DNA damage repair proteins. Western blot analysis was performed on SF188 extracts transfected with NFκB siRNA (cocktail containing NFκB1/p50 siRNA and RELB siRNA) or both NFκB siRNA and FOXM1 siRNA for 72 hours. (**E**) Exogenous expression of NFκB and FOXM1 in SF188 cells. Western blot analysis of doxycline inducible SF188/HA-FOXM1b cells transfected with exogenous NFκB (Flag-RELB and Flag-p50) expression plasmids for 48 hours. FOXM1 expression was induced 24 hours post transfection as indicated.

Supplementary Tables:

Supplementary Table S1. siRNA used in the study. All siRNAs were purchased from Thermo Fisher Scientific. All sequences are provided in 5' to 3' orientation.

Target gene	siRNA type	Sequence
RAD51	Stealth	GAGCUUGACAAACUACUUC
XRCC6/KU70	Stealth	GGAAGAGATAGTTTGATTT
Ligase IV	Stealth	GCACAAAGATGGAGATGTA
NFKB1/p50	Stealth	GCAGAUGGCCCAUACCUUCAAAUAU
NFKB1/p50	Stealth	GCACGAAUGACAGAGGCGUGUAUAA
RELB	Stealth	GCCCGUCUAUGACAAGAAATT
FOXM1	Stealth	CCCUGCCCAACAGGAGUCUAAUCAA
FOXM1	Stealth	GCCAUGAUACAAUUCGCCAUCAACA
Scramble (Scr)	Stealth	Medium GC content from Invitrogen

Supplementary Table S2. Primers used in real time PCR reactions to measure mRNA expression. All sequences are provided in 5' to 3' orientation.

Target gene	Orientation	Sequence
P21/CDKN1a	Forward	GAGACTAAGGCAGAAGATGTAGAG
	Reverse	GCAGACCAGCATGACAGAT
KU80/XRCC5	Forward	CAT GAA GAT GGA CCT ACA GCT AA
	Reverse	GGA AGT TTT CAG CAG GAT TCA C
KU70/XRCC6	Forward	TCA GAG TGA AGA TGA GTT GAC AC
	Reverse	ATA GAA CAC CAC AGC CAA GAG
DNAPKcs/ PRKDC	Forward	TGC CAT TGA TCA CCT ATG CC
	Reverse	AAA GCC ACT TGA CCA GAT CC
XLF/NHEJ1	Forward	GAT TGA AGA CAG AAC CAT TTG AAG A
	Reverse	GTG ACT GCC ATA TAC AGA TCC TG
LIG4	Forward	CAC AGA GGT AAC GGA GCT TG
	Reverse	TCT GTA TTC GTT CTA AAG TTG AAC AC
XRCC4	Forward	GCT GAT ACT CTC ATT GGT TGC
	Reverse	GGT GGA TTC TGC TTA TTT TTC TCT
POLQ	Forward	TAT CTG CTG GAA CTT TTG CTG A
	Reverse	CTC ACA CCA TTT CTT TGA TGG A
RAD51	Forward	CAG ACT ACT CGG GTC GAG GT
	Reverse	TCC ACT TGA GCT ACC ACC TG
BRCA1	Forward	GGT GGT ACA TGC ACA GTT GC
	Reverse	ACT CTG GGG CTC TGT CTT CA
BRCA2	Forward	GCC AAG TCA TGC CAC ACA TT
	Reverse	TGT GCC ATC TGG AGT GCT TT
FANCD2	Forward	CAA ACA GAA TGA AGC CAG CA
	Reverse	CCA TGG TCA CAG CAC CAA TA
MRE11a	Forward	TCC TAA AGT AAC CCA AGC CAT AC
	Reverse	TCC ACT ATA GTC CAC TCG CA
CHEK1	Forward	AGT ACT GTA GTG GAG GAG AGC
	Reverse	CCA ATA CCA TGC AGA TAA ACC AC
WEE1	Forward	TGG AGA TCA ATG GCA TGA AA
	Reverse	TAC CAG TGC CAT TGC TGA AG
NFKB1/p50	Forward	CAG GAG ACG TGA AGA TGC TG

	Reverse	AGT TGA GAA TGA AGG TGG ATG A
NFKB2/p52	Forward	CCA TCC ATG ACA GCA AAT CTC
	Reverse	AAC CGA ACC TCA ATG TCA TCT
RELA/p65	Forward	CGA GCT TGT AGG AAA GGA CTG
	Reverse	TGA CTG ATA GCC TGC TCC AG
RELB	Forward	ATG AAT GTG GTG AGG ATC TGC
	Reverse	AGC TCT GAT GTG TTT GTG GAT
c-REL	Forward	TTC CTC CTG TTG TCT CGA AC
	Reverse	TCC TCC TCT GAC ACT TCC AC
FOXM1	Forward	GGA GGA AAA GGA GAA TTG TCA C
	Reverse	GAT GGC GAA TTG TAT CAT GGC
FOXP3	Forward	CTA CTT CAA GTT CCA CAA CAT GC
	Reverse	CCA GTG GTA GAT CTC ATT GAG TG
FOXO1	Forward	GGA TAA GGG TGA CAG CAA CAG
	Reverse	TCC AGT TCC TTC ATT CTG CAC
18S	Forward	GAG ACT CTG GCA TGC TAA CTA G
	Reverse	GGA CAT CTA AGG GCA TCA CAG

Supplementary Table S3. Primers used for real time PCR following Chromatin Immunoprecipitation (ChIP-PCR). All sequences are provided in 5' to 3' orientation.

Target gene	Orientation	Sequence
P21/CDKN1a promoter	Forward	AGAAGAGGCTGGTGGCTATT
	Reverse	TGGGGTCTTTAGAGGTCTCC
P21/CDKN1a gene body	Forward	GCCGAAGTCAGTTCCTTGT
	Reverse	CTCTCACCTCCTCTGAGTGC
KU80/XRCC5	Forward	CTA CGG CGG AAT GGA GAG AA
	Reverse	CCC CGG AAC TCT GAG CAT
KU70/XRCC6	Forward	CAG GTC GTA CAC GTA GAG CT
	Reverse	GGG TAC GGG AAG GTC CAA G
XLF/NHEJ1	Forward	GGA GCA AAG AGG AAG GGA TA
	Reverse	CTT CTC TGC ATC CAT TTT CC
RAD51	Forward	GAC GGC AAC TCG GTT AAG TC
	Reverse	CGT CTG AGC CTA GGA GTT CG
CHEK1	Forward	ACA CCG GAT GCC ACT TCA TA
	Reverse	GGG AGA GAT CCT GGC TGA AG
WEE1	Forward	GGG TTC CCG CCA AAA TCG
	Reverse	GCA GCT CCG GGT TTG AAA A
Intergenic region	Forward	CCA CCA TGC CCA GCC TAA TA
	Reverse	AAT GTC TGG GCT CTC TCA CG

Supplementary Table S4. Statistical analysis of significance for the pairwise comparison of 53BP1 and γ-H2AX and RAD51 and γ -H2AX staining for each time point presented in Figure 3B-C. One-way standard ANOVA was performed followed by Newman-Keuls test to correct for multiple comparisons. Post-hoc pairwise comparisons were performed only if ANOVA p-value is <0.05.

FIGURE 3B	CUDC-907	RT	CUDC-907 + RT	KU70 siRNA + RT
53BP1 foci analysis at 3 hour time-point (ANOVA p<0.0001)				
Control	0.694094	0.000209	0.000210	0.000183
CUDC-907		0.000180	0.000183	0.000209
RT			0.353156	1.000000
CUDC-907 + RT				0.178259
53BP1 foci analysis at 24 hour time-point (ANOVA p=0.0005)				
Control	0.795071	0.295122	0.004459	0.002152
CUDC-907		0.216062	0.005323	0.003604
RT-24hr			0.001526	0.001229
CUDC-907 + RT				0.913279
γ–H2AX foci analysis at 3 hour time-point (ANOVA p<0.0001)				
Control	0.001133	0.000180	0.000183	0.000209
CUDC-907		0.000209	0.000210	0.000183
RT			0.934854	1.000000
CUDC-907 + RT				0.733696
γ–H2AX foci analysis at 24 hour time-point (ANOVA p<0.0036)				
Control	0.795071	0.295122	0.004459	0.002152
CUDC-907		0.216062	0.005323	0.003604
RT-24hr			0.001526	0.001229
CUDC-907 + RT				0.913279

FIGURE 3C	CUDC-907	RT	CUDC-907 + RT	KU70 siRNA + RT
RAD51 foci analysis at 3 hour time-point (ANOVA p<0.0001)				
Control	0.122120	0.000323	0.193697	0.070444
CUDC-907		0.000201	0.030471	0.009208
RT			0.000512	0.000736
CUDC-907 + RT				0.273001
RAD51 foci analysis at 24 hour time-point (ANOVA p=0.1357). No post-hoc Newman-Keuls test performed.				
γ–H2AX foci analysis at 3 hour time-point (ANOVA p<0.0001)				
Control	0.065836	0.000180	0.000209	0.000183
CUDC-907		0.000209	0.000183	0.000210
RT			0.897140	0.205458
CUDC-907 + RT				0.118281
γ–H2AX foci analysis at 24 hour time-point (ANOVA p<0.0001)				
Control	0.180807	0.282434	0.000481	0.010847
CUDC-907		0.861042	0.001363	0.056763
RT-24hr			0.000996	0.032293
CUDC-907 + RT				0.013171

Supplementary Table S5. Statistical analysis of significance for the pairwise comparison of mRNA expression data presented in Figure 4A. One-way standard ANOVA was performed followed by Newman-Keuls test to correct for multiple comparisons.

	Control vs CUDC-907	Controls vs RT	Controls vs CUDC-907 + RT	CUDC-907 vs RT	CUDC-907 vs CUDC-907 + RT	RT vs CUDC-907 + RT
KU80/XRCC5	0.008904	0.000226	0.015779	0.000231	0.336719	0.000201
KU70/XRCC6	0.003638	0.012599	0.017708	0.000391	0.109836	0.000840
DNAPKcs/PRDKC	0.081448	0.000223	0.377414	0.000231	0.150209	0.000201
XLF/NHEJ1	0.000579	0.205049	0.000397	0.000381	0.804905	0.000310
LIG4	0.008980	0.245880	0.000484	0.022607	0.008296	0.000759
XRCC4	0.030617	0.800071	0.658138	0.045590	0.036008	0.857300
POLQ	0.178890	0.080357	0.343108	0.017131	0.358874	0.040072
RAD51	0.000201	0.061237	0.000223	0.000231	0.011763	0.000201
BRCA1	0.005994	0.001571	0.011463	0.000276	0.299581	0.000287
BRCA2	Tests not performed as ANOVA did not yield a significant p value					
FANCD2	0.000215	0.000223	0.000228	0.000231	0.771589	0.000201
MRE11a	0.138000	0.005720	0.105721	0.030594	0.504092	0.037318
CHEK1	0.000201	0.000369	0.000223	0.000231	0.7	0.000201
WEE1	0.000201	0.000223	0.000223	0.000231	0.731608	0.000201

Supplementary Table S6. P value for all pairwise comparison on expression data presented in Figure 5A determined by one-way standard ANOVA followed by Newman-Keuls test to correct for multiple comparisons.

	Control vs CUDC-907	Controls vs RT	Controls vs CUDC-907 + RT	CUDC-907 vs RT	CUDC-907 vs CUDC-907 + RT	RT vs CUDC-907 + RT
NFKB1/p50	0.000201	0.000223	0.000223	0.000231	0.923065	0.000201
NFKB2/p52	0.005923	0.004392	0.000231	0.396586	0.000201	0.000223
RELA/p65	0.051491	0.928756	0.056199	0.025364	0.785567	0.039056
RELB	0.112100	0.000201	0.030170	0.000231	0.005717	0.000223
c-REL	0.039884	0.011862	0.079475	0.001254	0.344881	0.002089
FOXM1	0.000201	0.046310	0.000223	0.000231	0.555778	0.000201

Supplementary Table S7. Results of the one-way ANOVA followed by Newman-Keuls test on the chromatin immunoprecipitation data presented in Figure 5F.

Anti-RELB ChIP-PCR

	Control vs CUDC-907	Controls vs RT	Controls vs CUDC-907 + RT	CUDC-907 vs RT	CUDC-907 vs CUDC-907 + RT	RT vs CUDC-907 + RT
KU70	0.132556	0.011062	0.064069	0.002731	0.966372	0.001704
KU80	0.018026	0.000295	0.011739	0.000209	0.392243	0.000237
XLF	0.689566	0.000229	0.541048	0.000246	0.84456	0.000211
RAD51	0.312273	0.000269	0.282482	0.00028	0.688063	0.000249
WEE1	0.007364	0.014558	0.009311	0.000573	0.652798	0.000617
CHEK1	0.029012	0.019634	0.078409	0.001401	0.259441	0.003032
Intergenic region	Tests not performed as ANOVA did not yield a significant p value					

Anti-FOXM1 ChIP-PCR

	Control vs CUDC-907	Controls vs RT	Controls vs CUDC-907 + RT	CUDC-907 vs RT	CUDC-907 vs CUDC-907 + RT	RT vs CUDC-907 + RT
KU70	0.005799	0.000223	0.007914	0.000231	0.405032	0.000201
KU80	0.299326	0.000223	0.20442	0.000231	0.831586	0.000201
XLF	0.869152	0.000223	0.634402	0.000231	0.988815	0.000201
RAD51	0.463756	0.000223	0.381747	0.000231	0.760262	0.000201
WEE1	0.005803	0.000223	0.000203	0.000201	0.000278	0.000231
CHEK1	0.656925	0.000223	0.457737	0.000231	0.909969	0.000201
Intergenic region	0.405925	0.285597	0.032365	0.468911	0.069162	0.097431

Supplementary Table S8. The pairwise comparison p value for the mRNA expression presented in Figure 6B derived by one-way ANOVA followed by Newman-Keuls test.

	Scr vs NFκB + FOXM1 siRNA	Scr vs NFκB siRNA	NFκB siRNA vs NFκB +FOXM1 siRNA
XRCC6/KU70	0.002088	0.029342	0.014974
XRCC5/KU80	0.000524	0.020441	0.001799
XLF	0.000227	0.000252	0.000235
RAD51	0.002088	0.029342	0.014974
WEE1	0.023015	0.025229	0.478784
CHEK1	0.000235	0.816661	0.000227
XRCC4	0.018096	0.370299	0.025237
NFKB1/p50	0.000299	0.002268	0.001819
RELB	0.000227	0.000571	0.000235
FOXM1	0.000227	0.026063	0.000236